Journal of Neuroinflammation

RESEARCH

Open Access

CB2 expression in mouse brain: from mapping to regulation in microglia under inflammatory conditions

Wanda Grabon[1,2*†], Anne Ruiz[3†], Nadia Gasmi[1,2], Cyril Degletagne[4], Béatrice Georges[1,2], Amor Belmeguenai[1,2], Jacques Bodennec[1,2], Sylvain Rheims[1,2], Guillaume Marcy[5†] and Laurent Bezin[1,2*†]

Abstract

Since its detection in the brain, the cannabinoid receptor type 2 (CB2) has been considered a promising therapeutic target for various neurological and psychiatric disorders. However, precise brain mapping of its expression is still lacking. Using magnetic cell sorting, calibrated RT-qPCR and single-nucleus RNAseq, we show that CB2 is expressed at a low level in all brain regions studied, mainly by few microglial cells, and by neurons in an even lower proportion. Upon lipopolysaccharide stimulation, modeling neuroinflammation in non-sterile conditions, we demonstrate that the inflammatory response is associated with a transient reduction in CB2 mRNA levels in brain tissue, particularly in microglial cells. This result, confirmed in the BV2 microglial cell line, contrasts with the positive correlation observed between CB2 mRNA levels and the inflammatory response upon stimulation by interferon-gamma, modeling neuroinflammation in sterile condition. Discrete brain CB2 expression might thus be up- or down-regulated depending on the inflammatory context.

Highlights

- Tissue level of CB2 receptor mRNA is low and uniform across the various brain regions examined.
- The use of transcription and translation inhibitors during brain dissociation and cell sorting is efficient to prevent microglia *ex vivo* activation.
- CB2 mRNA was detected in scarce cells at the physiological state, was mainly detected in microglia and in some neurons.
- CB2 expression is downregulated in microglia during LPS-induced inflammatory peak and upregulated during the resolution of inflammation.
- LPS and IFNγ stimulation differently regulate CB2 expression in microglia.

Keywords Cannabinoid receptor type 2, Endocannabinoid system, Microglia, Neuroinflammation

†Wanda Grabon, Anne Ruiz, Guillaume Marcy and Laurent Bezin contributed equally.

*Correspondence:
Wanda Grabon
wanda.grabon@univ-lyon1.fr
Laurent Bezin
laurent.bezin@univ-lyon1.fr
Full list of author information is available at the end of the article

Introduction

The function of cannabinoid receptor type 2 (CB2), mainly expressed by leukocytes, has initially been limited to its peripheral immunomodulatory role [1–3]. However, the use of CB2-specific ligands and the availability of CB2-Knock Out (KO) mice have unveiled its potential role in central nervous system (CNS) functions under both physiological and pathological conditions [4, 5]. To gain deeper insights into its involvement in brain functions, it is essential to identify the cells targeted by its ligands, a pursuit that holds significant therapeutic promise in neuropsychiatric and neuroinflammatory diseases [6, 7]. Nevertheless, precise and accurate mapping of cnr2 gene expression remains difficult to establish on the basis of CB2 protein detection, mainly because specific antibodies are still lacking [8–10]. The detection of CB2 transcript is therefore today the reference technique to overcome the issue of antibody specificity, providing both highly sensitive and specific quantification. The presence of CB2 mRNA was previously investigated and reliably detected in a few isolated regions, namely in the ventral tegmental region (VTA)[11, 12], striatum [13–15] and hippocampus [13, 16, 17].

The primary goal of this study was to quantify and compare at the tissue level with calibrated RT-qPCR CB2 expression and other primary cannabinoid receptors, CB1, GPR18, and GPR55, across eleven major brain regions in three different mouse strains (C57Bl/6, Balb/c, and Swiss). The second objective of this study was to determine which cell types predominantly support CB2 expression in the brain. We used cell sorting techniques from dissociated adult brain tissue to determine CB2 mRNA level in populations enriched in microglia and neurons, but also in astrocytes/oligodendrocytes and in endothelial cells. To reach this objective, we took a particular attention in limiting microglial cell activation throughout the whole technical procedures using transcriptional and translational inhibitors [18]. Furthermore, we took advantage of access to a single-nucleus database obtained from cortex tissue collected from 10-day- old mice to assess what might be the proportion of cells expressing CB2 in each cell populations.

CB2 expression is known to be regulated as a function of inflammatory state [19, 20]. Indeed, CB2 expression in brain tissue has been shown to be induced in neurological conditions associated with an inflammatory state, such as stroke, traumatic brain injury or Alzheimer's disease [5, 7]. Most studies suggest that microglial cell activation is responsible for this induction. But intriguingly, few in vitro studies in which non-sterile neuroinflammation is modelled by lipopolysaccharide (LPS) stimulation of microglial cells report a down-regulation of CB2 [20, 21]. Our third objective was to better understand whether CB2 expression is similarly coordinated with inflammatory markers after a sterile or non-sterile inflammatory challenge, modeled by stimulation with interferon-gamma (IFNγ) or LPS, respectively, known to activate different inflammatory intracellular signaling pathways [22, 23]. Our study is the first to demonstrate that CB2 gene expression in the brain is supported by a very small number of microglial cells, and by neurons in even smaller proportions, and that microglial CB2 transcript levels can be up- or down-regulated depending on the inflammatory context and timing.

Results

CB2 expression in basal condition is consistent across brain regions with minimal strain variability

Tissue transcript levels of CB2 and 3 other cannabinoid receptors—CB1, GPR18 and GPR55—were determined in eleven microdissected regions from the adult (8-week-old) mouse brain: olfactory bulb, neocortex, hippocampus, hypothalamus, cerebellum, brainstem, ventral limbic region (VLR, comprising the amygdala, agranular insular cortex and piriform cortex), nucleus accumbens, substantia nigra, striatum and VTA (Fig. 1A). Comparative analysis of cannabinoid receptor mRNA levels was performed across three commonly used mouse strains: C57bl/6, Balb/c and Swiss (n = 3–4/group). Transcripts of the 4 receptors were detected in all mouse strains and in all brain regions. CB2 expression was not significantly different between mouse strains in the 11 regions investigated (Table S2). For the other 3 receptors—CB1, GPR55 and GPR18—only 10 isolated inter-strain differences were measured out of the 99 comparisons made (3 strains, 11 structures, 3 receptors, Table S2). To compare the expression of CB2 with the other cannabinoid receptors in the different regions, data from the 3 mouse strains were combined. For CB2 transcripts, no significant inter-region difference was observed, except for levels measured in the VTA, that were significantly lower than those of the olfactory bulb ($p < 0.0001$), the hippocampus ($p = 0.0051$), the VLR ($p = 0.0136$) and the substantia nigra ($p = 0.0002$) (Fig. 1B). It should be noted that the distribution of transcript levels of the other cannabinoid receptors is much less homogenous (Kruskall Wallis: CB1, GPR18, GPR55: $p < 0.0001$, Fig. S2).

CB2 was expressed at much lower levels than other endocannabinoid receptors in all regions studied (Fig. 1C–M). Overall, CB1 and GPR18 were the two most expressed cannabinoid receptors among the investigated regions, and GPR55 was expressed at intermediate levels.

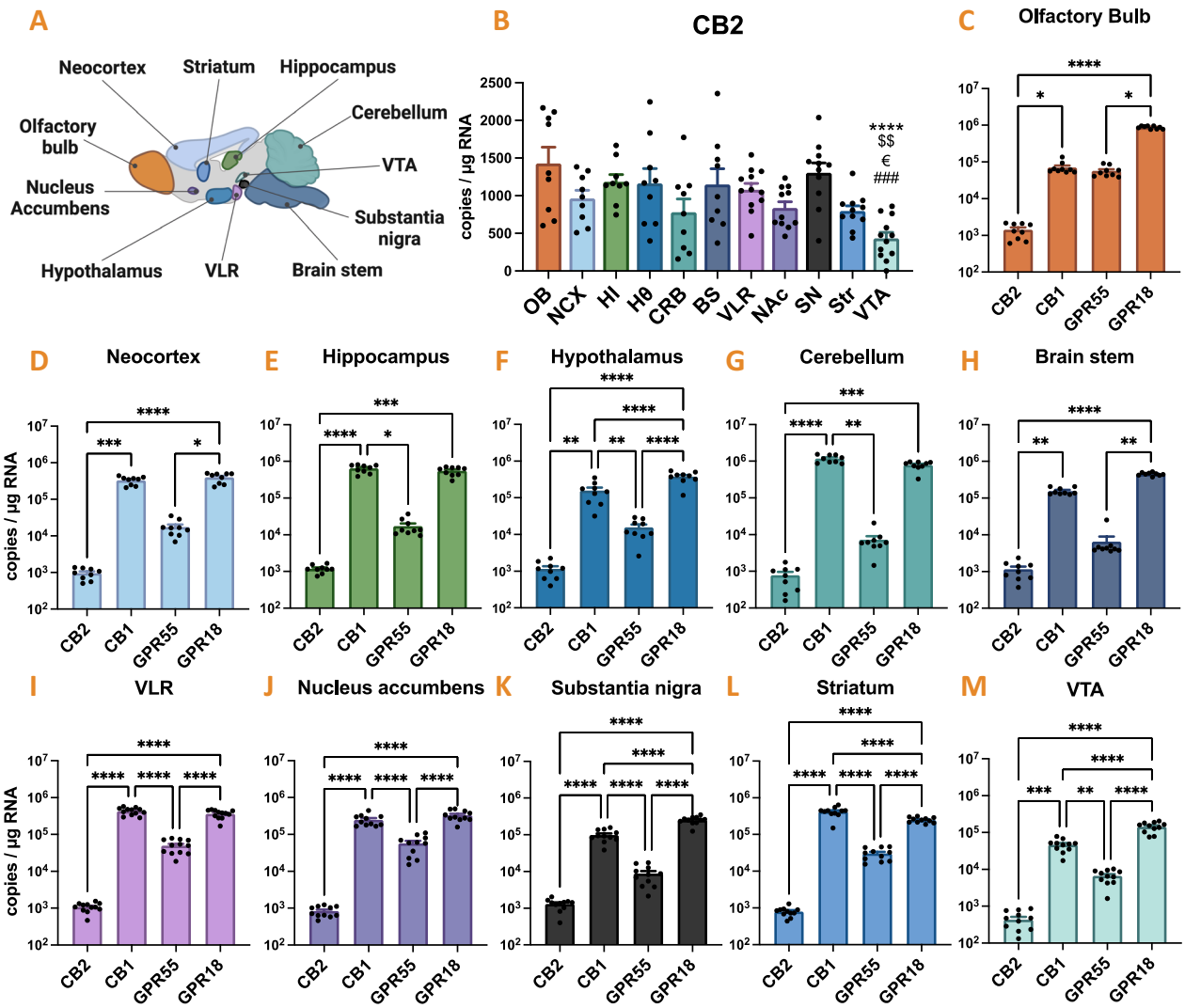

Fig. 1 Regional distribution of cannabinoid receptors mRNA in the healthy mouse brain. CB2 mRNA was quantified using calibrated RT-qPCR and compared with other cannabinoid receptors CB1, GPR18 and GPR55 in eleven microdissected regions from adult mouse brain: the olfactory bulb (OB), the neocortex (NCX), the hippocampus (HI), the hypothalamus (Hθ), the cerebellum (CRB), the brainstem (BS), n = 9 mice; the ventral limbic region (VLR), the nucleus accumbens (NAc), the substantia nigra (SN), the striatum (Str) and the ventral tegmental region (VTA), n = 12 mice. **A** Representation of the 11 microdissected regions. **B** Quantification of CB2 transcript levels. Tukey's tests following one-way ANOVA: *, VTA vs. OB: $p < 0.0001$; $, VTA vs. HI: $p = 0.0051$; €, VTA vs. VLR: $p = 0.0136$; #, VTA vs. SN: $p = 0.0002$. **C–M** Quantification of CB2, CB1, GPR18 and GPR55 in each microdissected region. Transcript levels are expressed as copies of cDNA per microgram of total RNA. Values are presented as means + SEM. Normal data were analyzed with Tukey's post-hoc test for multiple comparisons following one-way ANOVA (Hθ, VLR, NAc, SN, Str, VTA: $p < 0.0001$). Non-normal data were analyzed with Dunn's post-hoc test for multiple comparisons following Kruskal–Wallis test (OB: $p < 0.0001$, NCX: $p < 0.0001$, HI: $p < 0.0001$, CRB: $p < 0.0001$, BS: $p < 0.0001$). *, $p < 0.05$; **, $p < 0.01$; ***, $p < 0.001$, ****, $p < 0.0001$. Not significantly statistical differences are not graphically represented

Transcription and translation inhibitors prevent microglia ex vivo activation during tissue dissociation and cell sorting

Ex vivo activation of brain cells, in particular microglial cells, can change the accuracy of measurements related to the inflammatory state within brain tissue. While this activation can be minimized by rapid microdissection on ice and immediate freezing of samples, it remains a concern during tissue dissociation protocols, involving heating, enzymes and mechanical damage, and during cell sorting protocols [18, 24]. To prevent this activation, buffers can be supplemented with transcriptional and translational inhibitors such as actinomycin D (ActD), triptolide (Trip), and anisomycine (Anis) [24]. Here, the efficacy of these inhibitors was tested in CD11b-enriched populations from adult C57Bl/6 mouse brains,

the purity of which reached 91.1% (Fig. 2A). Based on quantification of IL-1β and TNFα transcripts, when the buffer contained no inhibitor, the level of gene activation in microglial cells sorted from adult mouse brains was the highest (Fig. 2B, C). For the IL-1β transcript, inhibition of transcription alone using ActD resulted in a 47.4% decrease of expression level, while inhibition of both transcription and translation using the inhibitor cocktail decreased it much more strongly, with a 91.6% decrease (Fig. 2B). For the TNFα transcript, the only condition that led to a decrease in its expression level was the inhibitor cocktail (Fig. 2C). Our data support that inhibition of both transcription and translation, here applied as early as intracardiac perfusion, is necessary to limit the level of gene activation in microglial cells during tissue dissociation and cell sorting [24]. Therefore, to avoid any bias related to ex vivo activation of microglia, all further MACS studies were performed in the presence of the inhibitor cocktail from brain perfusion, to dissociation, cell labelling, and cell sorting.

CB2 mRNA expression in sorted brain cells shows peak levels in microglia at the physiological state

Different cell populations from mouse hippocampus and neocortex were enriched using MACS after tissue dissociation and subsequently immunophenotyped using flow cytometry (Fig. S3). High degrees of purity were measured, with 98.2% purity in cell population enriched in both astrocytes ($ACSA2^+/O4^-$: 64%) and oligodendrocytes ($O4^+$: 34.2%), 60.9% in a cell population enriched in $Ly6C^+/CD31^+$ endothelial cells, 98.2% in cell population enriched in $CD11b^+$ microglial cells, and 96.9% in the neuronal population negative for all tested flow cytometry cell markers. The identity of the enriched cell populations was further confirmed using RT-qPCR, by detecting and quantifying transcript level of various typical cell markers (Fig. 3A–D). Significant differences in CB2 mRNA levels were measured between the different enriched-cell populations (Fig. 3E). The highest CB2 mRNA expression was found in the microglia-enriched cell population, showing a tenfold increase compared to neuronal cell-enriched population and 63–153-fold increase compared to endothelial cells and astrocytes/oligodendrocytes, respectively.

We next performed a single nucleus RNA seq experiment on 10-day-old mice to estimate what might be the proportion of CB2-expressing cells in each of the populations enriched by MACS. Neonatal brain tissue has the advantage of being easy to dissociate for subsequent single-cell analysis, unlike adult tissue which contains a lot of debris due to myelin accumulation. Importantly, the stability of CB2 mRNA levels between neonatal brain and adulthood, in both hippocampus and neocortex (Fig. 3F), as previously described in the hippocampus [17], facilitated a meaningful comparison between the MACS data obtained at 8 weeks and the single-nucleus RNAseq data obtained at 10 days.

We isolated 10k nuclei, excluded low quality nuclei, clustered and annotated the cell types (Fig. 3H) based on classical markers (Fig. S4). We quantified that CB2 mRNA was detected in less than 1% of total cells, identified as neurons, microglia and astrocytes. The population

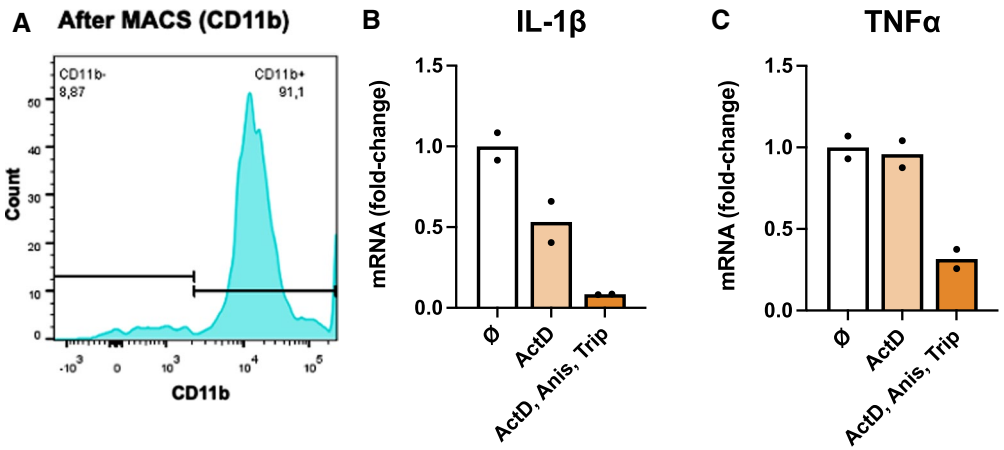

Fig. 2 Prevention of microglial activation during dissociation and cell sorting protocols using transcription and translation inhibitors. **A** Brain tissue from adult mice was dissociated using Miltenyi's ABDK protocol and CD11b-positive cells were enriched using MACS CD11b magnetic microbeads. Purity of CD11b-positive population was controlled on a pool of cells from each sample by cytometry. **B, C** IL-1β (**B**) and TNFα (**C**) mRNAs were quantified using calibrated RT-qPCR following tissue dissociation and CD11b MACS cell enrichment from adult mouse brain (n = 2). Dissociation and MACS protocols were performed with classic buffer (ø), with buffer complemented with transcription inhibitor ActD (3 µM) or with buffer complemented with both transcription and translation inhibitors ActD, Anis and Trip (3 µM, 100 µM and 10 µM, respectively). Transcript levels are expressed as fold change of the classic buffer (ø) condition. Individual values (dots) and average values (bars) are presented

with the highest proportion of CB2-positive cells was microglia, with a proportion around 20-fold greater than in neurons and tenfold greater than in astrocytes. CB2-expressing nuclei are visualized in red in Fig. 3I.

CB2 mRNA levels in the neocortex and the hippocampus following LPS

LPS administration in adult C57Bl/6 mice led to a significant inflammatory peak at 3h as reflected by high levels of TNFα, IL-1β, IL-6, COX2, NOS2 and MCP1 transcripts in the hippocampus and neocortex (Fig. 4A–F). The inflammatory index calculated from the transcript levels of these pro-inflammatory genes peaked at 13.2-fold ± 1.6 the control level (Fig. 4G). The amounts of CB2 transcript 3h after LPS administration, i.e. during the inflammatory peak, transiently decreased to 52 ± 9% of those in controls, before rebounding 24h later, to 194 ± 19% above controls, once inflammation had resolved (Fig. 4H). The level of CB2 transcript was inversely correlated to the inflammatory index after administration of LPS (Fig. 4I). Conversely, CB1 and GPR18 transcript levels were uncorrelated, while those of GPR55 were positively correlated with the inflammatory index (Fig. S5).

CB2 mRNA levels in microglia following LPS

In these experiments, all steps were performed with buffers complemented with inhibitor cocktail. Brains were collected 3 h or 24 h post-LPS treatment. Total RNAs were extracted from MACS sorted CD11b-enriched cell populations, whose purity, estimated by cytometry, ranged between 85.7% and 98.7% (Fig. 5A). As measured in tissue homogenates, LPS administration led to a significant inflammatory peak in microglial cells at 3h as reflected by high levels of TNFα, IL-1β, IL-6, COX2, NOS2 and MCP1 transcripts (Fig. 5B–G). The calculated pro-inflammatory index peaked at 43.2-fold ± 6.4 the control level (Fig. 5H). CB2-mRNA level present in microglial cells 3h after LPS administration transiently were reduced by 84.4 ± 7.4%, before rebounding 24h later, 171 ± 19% above controls, once inflammation had resolved (Fig. 5I). The level of CB2 transcript was inversely correlated to the pro-inflammatory index after administration of LPS (Fig. 5J). Conversely, GPR55 and GPR18 transcript levels were not significantly correlated with the pro-inflammatory index (Fig. S6).

CB2 mRNA levels in microglia BV2 cell line following LPS or IFNγ stimulation

Based on the quantification of pro-inflammatory gene transcripts (Fig. 6A–F) and the calculation of the pro-inflammatory index (Fig. 6G), LPS treatment of murine BV2 microglial cells led to an inflammatory response that peaked between 2 and 4h. At the same time, CB2-mRNA levels were reduced by 92 ± 0.7%2h after LPS treatment compared to untreated cells (Fig. 6H). As for levels measured in brain tissue and microglia sorted cells, CB2-mRNA level was inversely correlated with the pro-inflammatory index (Fig. 6I). GPR55-mRNA levels were also inversely correlated with the pro-inflammatory index while GPR18 expression was not regulated during LPS-induced inflammation (Fig. S7).

Previous studies have shown that stimulation of BV2 cells with IFNγ resulted in a reverse regulation of CB2 expression compared to that induced by LPS [20]. Komorowska-Müller et al. hypothesized that this difference in regulation could be due to a much lower level of inflammation after IFNγ compared to LPS, and to different nature of the two stimuli, IFNγ being a cytokine released during sterile inflammation, and LPS a bacterial toxin [7].

IFNγ treatment of BV2 cells led to an increase in most pro-inflammatory gene transcripts, except for IL-1β, (Fig. 7A–F) and of the pro-inflammatory index (Fig. 7G), that peaked at 8h. The level of inflammation was mostly resolved by 24h. Interestingly, CB2-mRNA levels did not drop but increased up to twofold during

(See figure on next page.)

Fig. 3 Cell distribution of CB2 mRNA in the mouse brain. **A–E** Adult mouse brain tissue was dissociated as in Fig. 2. Four populations were enriched by MACS technique. Expression of specific cell markers was quantified by RT-qPCR to control for cell population identity and purity: **A** Neurons, expressing NeuN mRNA; **B** CD11b-positive microglia, expressing CD115 and Iba1 mRNA; **C** Ly6C-positive endothelial cells, expressing CD31 and Ly6C mRNA; **D** ACSA2-positive astrocytes and oligodendrocytes, expressing GFAP and GLAST mRNA. **E** CB2 mRNA was quantified using calibrated RT-qPCR in the four MACS-enriched cell populations. Transcript levels are expressed as copies of cDNA per µg of total RNA reverse transcribed. Values are presented as mean + SEM, analyzed with Tukey's test for multiple comparisons following one-way ANOVA. 554,052 ± 92,463 CB2 cDNA copies/µg RNA were quantified in microglia-enriched cell population. Microglia vs. Neurons: $p = 0.0004$; Microglia vs. Astro/oligo: $p = 0.0002$; Microglia vs. Endothelial cells: $p = 0.0002$. **F**. Levels of CB2 transcripts quantified at tissue level in the hippocampus (HI) and neocortex (NCX) are expressed as % of the mean calculated in respective adult group. CB2 mRNA levels are similar in P10 (n = 8) and adult (P56) mice (n = 6), analyzed with Tukey's test for multiple comparisons following one-way ANOVA. HI adult vs. P10: $p = 0.7796$; NCX adult vs. P10: $p = 0.6922$. **G.** Percentage of CB2-positive cells in clustered nuclei. Data are analyzed with Fisher exact test. Microglia vs. neurons, $p < 0.0001$; microglia vs. astrocytes: $p = 0.0114$. **H**. Clustering of Single nuclei sorted from P10 mice neocortices **I**. Visualization of CB2-expressing nuclei (red) among clustered sorted nuclei. Asterisks represent comparisons vs. microglia: *, $p < 0.05$; **, $p < 0.01$; ***, $p < 0.001$, ****, $p < 0.0001$

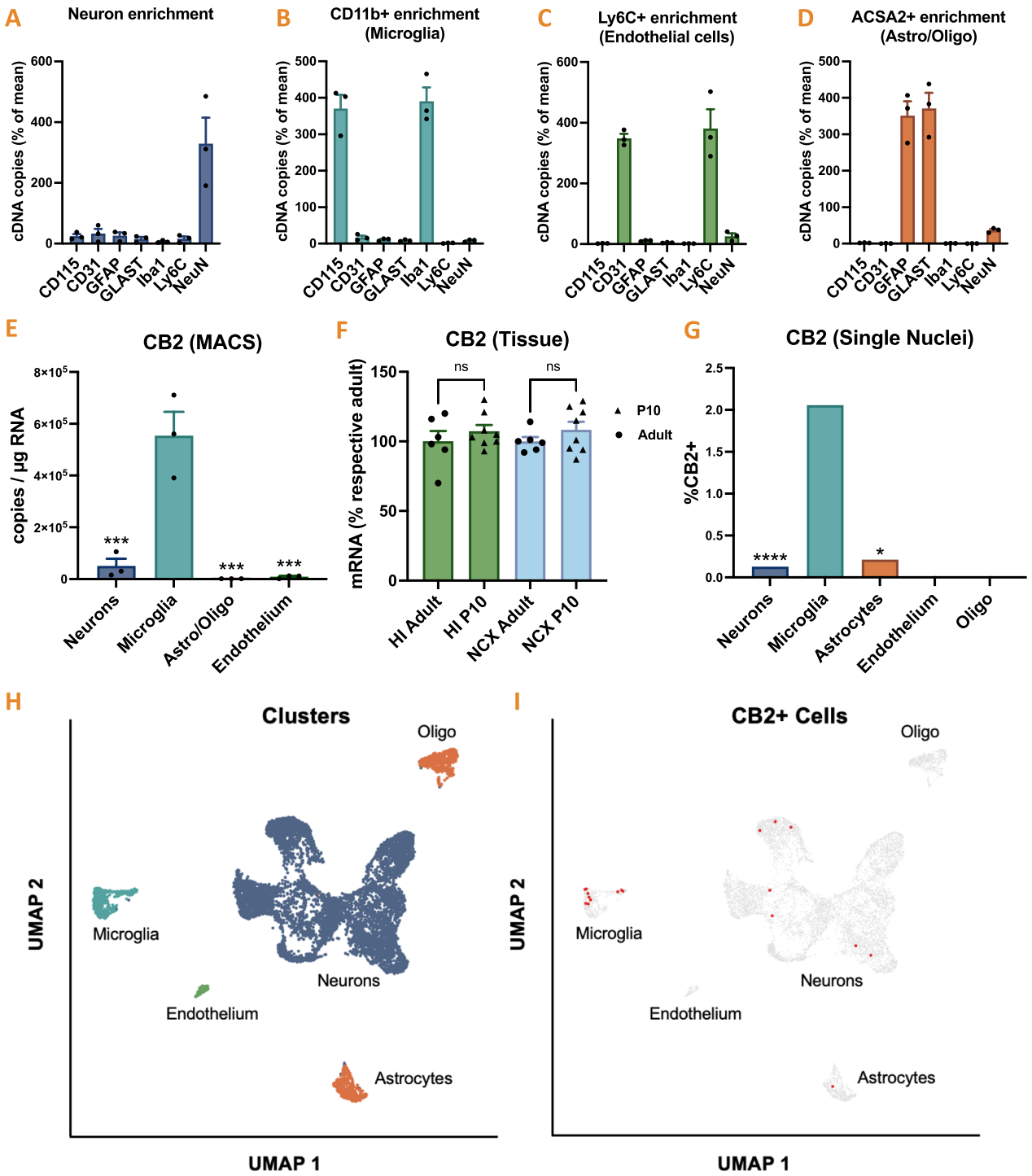

Fig. 3 (See legend on previous page.)

the inflammatory peak compared with untreated cells (Fig. 7H) and were positively correlated with the pro-inflammatory index (Fig. 7I). The main observed difference with LPS treatment was the absence of peak in IL-1β- transcripts following IFNγ treatment in BV2 cells (Fig. 7A).

To determine whether the dramatic decrease in CB2-mRNA level, observed only under LPS treatment, was

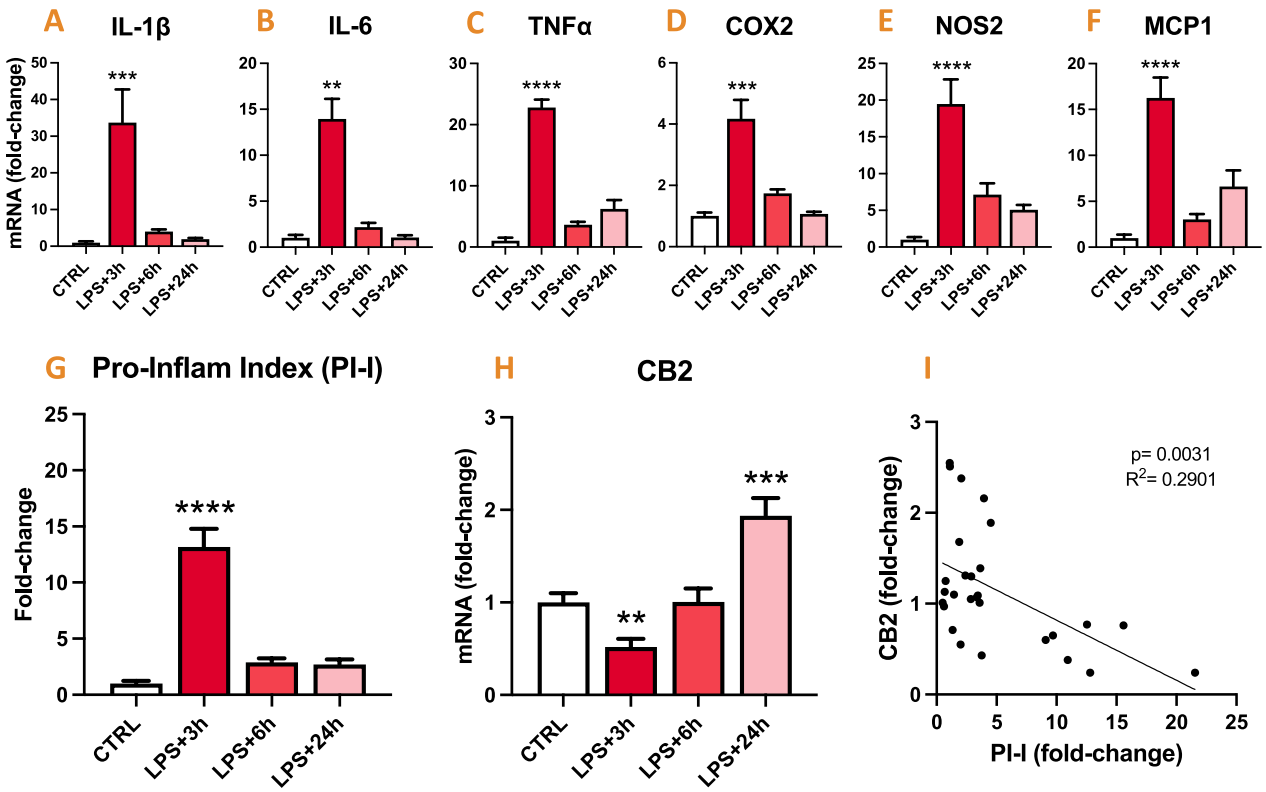

Fig. 4 CB2 mRNA inversely correlated with levels of inflammatory markers in brain after LPS challenge. Transcript levels of pro-inflammatory genes and CB2 were quantified in the neocortex and the hippocampus of adult C57Bl/6 mouse brains, 3h (n = 7), 6h (n = 7) and 24h (n = 8) following LPS administration (5 mg/kg, IP) and compared with untreated control (CTRL) mice (n = 6). **A–F** Quantification of IL-1β, IL-6, TNFα, COX2, NOS2 and MCP1 transcript levels. **G.** Pro-inflammatory index (PI-I) was calculated from transcript levels of pro-inflammatory genes (**A–F**). CTRL vs. LPS + 3h: $p < 0.0001$. **H** Quantification of CB2 mRNA. Data are expressed as the mean ± SEM, and presented as relative to control mice. CTRL vs. LPS + 3h: $p = 0.0036$; CTRL vs. LPS + 24h: $p = 0.0008$. Normal data (NOS2, MCP1, PI-I and CB2) were analyzed with Tukey's test following one-way ANOVA. Non-normal data (IL-1β, TNFα, IL-6, COX2) were analyzed with Dunn's test following Kruskal–Wallis test. Asterisks represent LPS-treated groups vs. CTRL: *, $p < 0.05$; **, $p < 0.01$; ***, $p < 0.001$, ****, $p < 0.0001$. **I** Relationship between CB2 transcript level and PI-I (simple linear regression, $p = 0.0031$, $R^2 = 0.2901$, $y = -0.06617x + 1.480$, $n = 28$)

(See figure on next page.)

Fig. 5 CB2 mRNA levels is inversely correlated with inflammatory markers in microglia after LPS administration. Brain tissue of adult C57Bl/6 mice was dissociated using Miltenyi's ABDK protocol and microglia-enriched cell population was sorted as in Fig. 2. Pro-inflammatory genes and CB2 mRNA were quantified by RT-qPCR in CD11b-positive cells sorted from mouse brain (neocortex and hippocampus) 3h (n = 5) and 24h (n = 5) following LPS administration (5 mg/kg, IP) and compared with untreated (CTRL) mice (n = 4). **A** The purity of the MACS-sorted CD11b-positive cells was estimated by quantifying the protein expression of CD11b by flow cytometry on a fraction of pooled cell suspensions harvested before and after CD11b MACS magnetic sorting. **B–G** Quantification of IL-1β, IL-6, TNFα, COX2, NOS2 and MCP1 transcript levels. **H.** Pro-inflammatory index (PI-I) was calculated from transcript levels of pro-inflammatory genes (**A–F**). CTRL vs. LPS + 3h: $p < 0.0001$. **I.** Quantification of CB2 mRNA. CTRL vs. LPS + 3h: $p = 0.0061$; CTRL vs. LPS + 24h: $p = 0.0132$. Data are expressed as mean + SEM, and presented as relative to microglia from control mice. Normal data (IL-1β, IL-6, COX2, MCP1, PI-I and CB2) were analyzed with Tukey's test following one-way ANOVA. Non-normal data (TNFα and NOS2) were analyzed with Dunn's test following Kruskal–Wallis test. Asterisks represent LPS-treated groups vs CTRL: *, $p < 0.05$; **, $p < 0.01$; ***, $p < 0.001$, ****, $p < 0.0001$. **J** Relationship between CB2-mRNA levels and PI-I (simple linear regression, $p = 0.0012$, $R^2 = 0.5962$, $y = -0.02596x + 1.423$, $n = 14$)

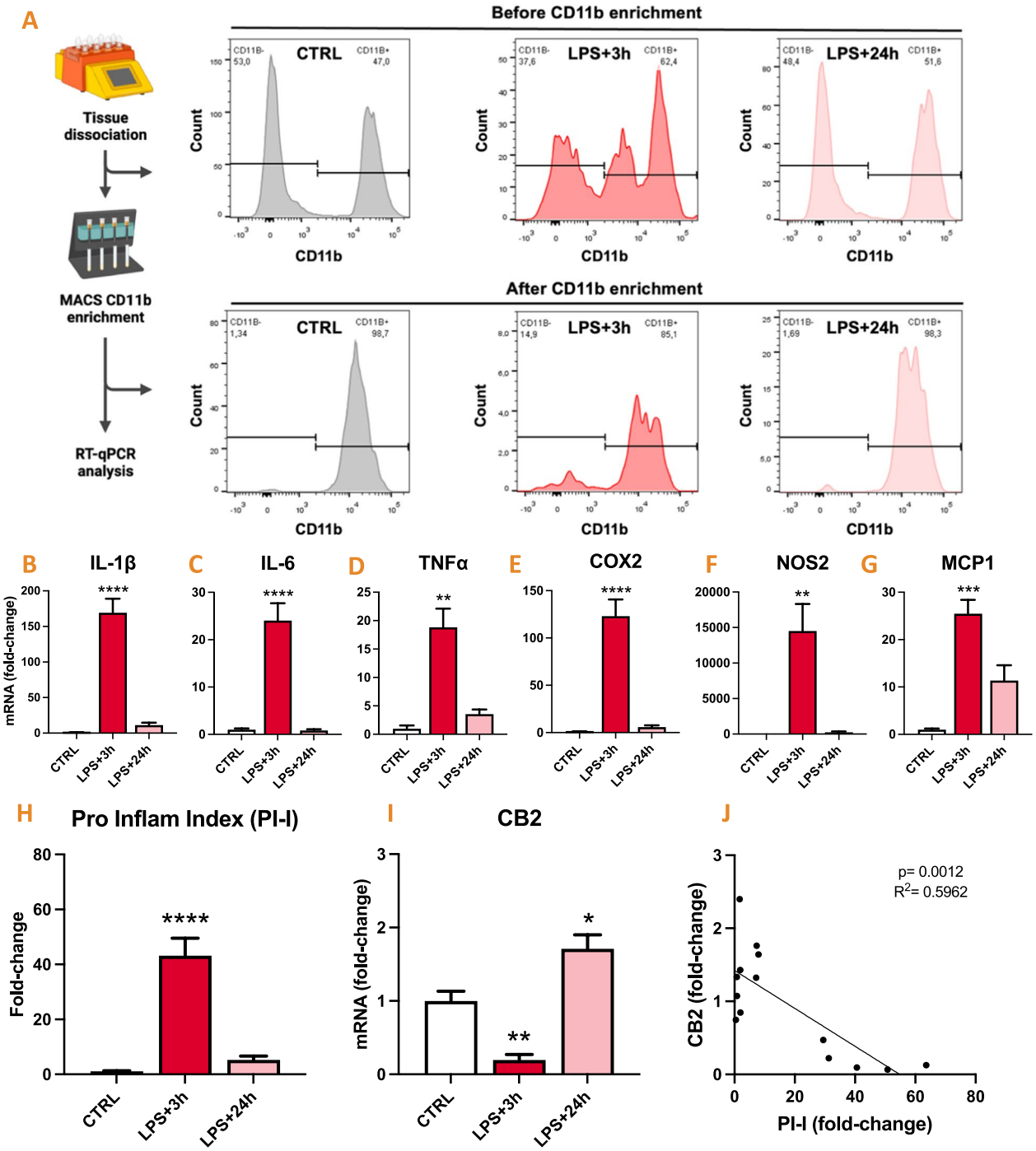

Fig. 5 (See legend on previous page.)

due to strong activation of IL-1R by IL-1β, BV2 cells were incubated with IL-1RA (1–1000 ng/mL), the natural IL-1R antagonist, 30-min prior to and during LPS. IL- 1RA did not prevent LPS-induced CB2 mRNA level decrease (Fig. S8).

Discussion

Main results

In this study, we demonstrated at the transcriptional level that the CB2 receptor exhibits consistently low and uniform expression across various brain regions examined,

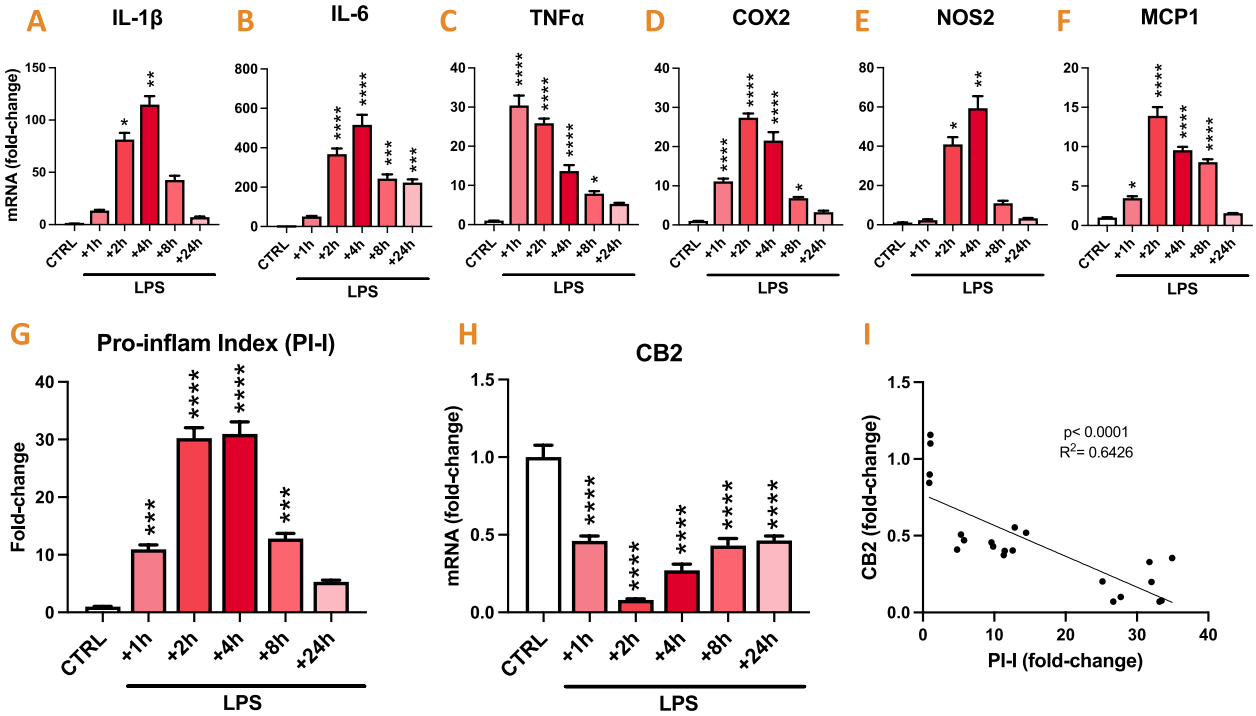

Fig. 6 CB2 mRNA levels inversely correlated with inflammatory markers in BV2 cells after LPS treatment. Inflammatory genes and CB2 mRNA were quantified by calibrated RT-qPCR in cultured BV2 murine cells following LPS 1 h, 2 h, 4 h, 8 h or 24 h application (100 ng/mL) and compared with levels quantified in untreated cells (CTRL, LPS + 1 h, + 2 h, + 4 h: n = 4/condition; LPS + 8 h, + 24 h: n = 3/condition). **A–F** Quantification of IL-1β, IL-6, TNFα, COX2, NOS2 and MCP1 transcript levels. **G** Pro-inflammatory index (PI-I) was calculated from transcript levels of pro-inflammatory genes (**A–F**). CTRL vs. LPS + 1h: p = 0.0005; vs. + 2h: p < 0.0001; vs. + 4h, p < 0.0001; vs. + 8h: p = 0.0002. **H.** Quantification of CB2-mRNA. CTRL vs. LPS + 1h: p < 0.0001; vs. + 2h: p < 0.0001; vs. + 4h, p < 0.0001; vs. + 8h: p < 0.0001; vs. + 24h: p < 0.0001. Data are expressed as the mean ± SEM, and presented as relative to untreated BV2 cells. Normal data (TNFα, IL-6, COX2, MCP1, PI-I and CB2) were analyzed with Tukey's test for multiple comparisons following one-way ANOVA. Non-normal data (IL-1β and NOS2) were analyzed with Dunn's test for multiple comparisons following Kruskal–Wallis test. Asterisks represent control (CTRL) vs. respective LPS-treated group. *, p < 0.05; **, p < 0.01; ***, p < 0.001, ****, p < 0.0001. **I** Relationship between CB2-mRNA levels and PI-I (simple linear regression, p < 0.0001, $R^2 = 0.6426$, y = − 0.02012x + 0.7688, n = 22)

including the olfactory bulb, neocortex, hippocampus, hypothalamus, cerebellum, brainstem, VLR, nucleus accumbens, substantia nigra, striatum and VTA. Notably, there were no significant differences in CB2 expression among the three mouse strains (C57bl/6, Balb/c, and Swiss) studied. Our findings highlighted that microglia are the primary cell type expressing CB2 in the brain, while neurons displayed lower levels of CB2 expression. Additionally, we noted an inverse relationship between CB2 expression and the degree of LPS-induced inflammation over time. This was evidenced by a decrease in CB2 transcript levels coinciding with the peak of inflammation, as observed both at the tissue level in the hippocampus and neocortex, as well as at the cellular level in sorted microglial populations and BV2 microglial cell line. Intriguingly, we observed the opposite relationship after stimulation of BV2 cells with IFNγ, which activates different intracellular pathways from LPS.

Methodological consideration

One of the objectives of the study was to determine which cell types contribute to the expression of CB2 measured in brain tissue, involving the use of cell sorting protocols. Obtaining a cell suspension from brain tissue and enriching cell populations by magnetic or fluorescent sorting represents an assault on brain cells that can alter their phenotypic state. Microglia are effective sentinels, continuously scanning the microenvironment in their basal state, and entering an extremely rapid activation process whenever cerebral homeostasis is compromised [25, 26]. Ex vivo microglial activation can introduce confounds that can distort measurements of the transcriptomic profile in basal state or mask endogenously induced activation, as in a pathological condition [24]. Previous studies have shown that supplementing the buffer with transcription and translation inhibitors during the enzymatic and mechanical dissociation of brain tissue limits ex vivo

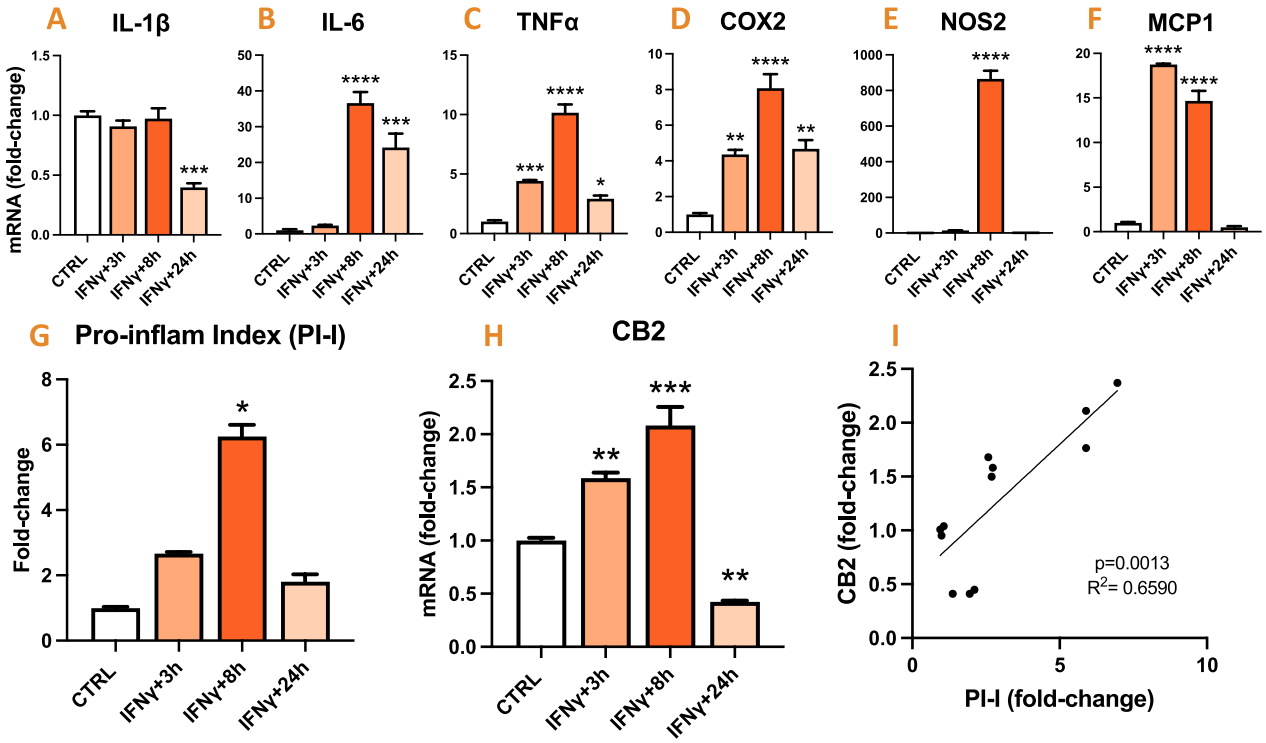

Fig. 7 CB2 mRNA levels positively correlated with inflammatory markers in BV2 cells after IFNγ treatment. Inflammatory genes and CB2 mRNA were quantified by calibrated RT-qPCR in cultured BV2 murine cells following IFNγ 3 h, 8 h or 24 h application (100 ng/mL) and compared with levels quantified in untreated cells (n = 3/condition). **A–F** Quantification of IL-1β, IL-6, TNFα, COX2, NOS2 and MCP1 transcript levels. **G** Pro-inflammatory index (PI-I) was calculated from transcript levels of pro-inflammatory genes (**A–F**). CTRL vs. IFNγ + 8h: p = 0.0132. **H** Quantification of CB2 mRNA. CTRL vs. IFNγ + 3h: p = 0.0088; CTRL vs. IFNγ + 8h: p = 0.0002; CTRL vs IFNγ + 24h: p = 0.0097. Data are expressed as the mean ± SEM, and presented as relative to untreated BV2 cells. Normal data (IL-1β, IL-6, TNFα, COX2, NOS2, MCP1 and CB2) were analyzed with Tukey's post-hoc test for multiple comparisons following one-way ANOVA. Non-normal data (PI-I) were analyzed with Dunn's post-hoc test for multiple comparisons following Kruskal–Wallis test. Asterisks represent control (CTRL) vs respective IFNγ-treated group. *, $p < 0.05$; **, $p < 0.01$; ***, $p < 0.001$, ****, $p < 0.0001$. **I** Relationship between of CB2 transcript levels and pro-inflammatory index (simple linear regression, p = 0.0013, $R^2 = 0.6590$, y = 0.2545x + 0.5265, n = 12)

activation of microglial cells [18]. Here, we showed that using the same inhibitors from intracardiac perfusion stage through to final cell collection indeed limited the induction of IL-1β and TNFα pro-inflammatory markers in microglial populations enriched from brain tissue of healthy adult mice. As sentinel cells of the CNS, microglial cells are the most likely to be sensitive to ex vivo activation during the cell dissociation and sorting protocol. Nevertheless, uncontrolled gene activation may also occur in other cell types during these steps. We only tested the effect of inhibitors on microglial cells and not on other cell populations. We have assumed that inhibition of non-physiological activation of microglia may also extend to other brain cell types, since the targets of transcriptional and translational inhibitors are conserved in all eukaryotic cell types [27, 28] and are therefore not cell-specific.

CB2 basal expression in the CNS

Under physiological conditions, we showed no inter-strain (C57bl/6, Balb/c and Swiss), nor any spatial regulation of *cnr2* gene expression according to the brain regions studied: the olfactory bulb, the neocortex, the hippocampus, the hypothalamus, the cerebellum, the brainstem, the VLR, the nucleus accumbens, the substantia nigra, the striatum and the VTA. The only region with a slightly lower level of CB2 expression than the other regions is the VTA, which is one of the areas in which CB2 is most studied, notably for its role in the reward system [11, 12], suggesting that the physiological role of CB2 is not limited to the dopaminergic system. CB2 transcript levels were relatively low when compared to other main cannabinoid receptors CB1, GPR18 and GPR55. Confirmation of the presence of CB2 in the physiological state is consistent with quantifiable

behavioral outcomes in healthy mice, for example on memory [29, 30], mood [31] or pain sensitivity [32, 33] measured after administration of CB2-specific ligands [5]. Given the very low number of CB2-positive cells measured by single nuclei, neurons and microglia expressing CB2 must establish major connections with the neuronal networks controlling the brain functions studied.

The homogeneity of CB2 expression contrasts with the great heterogeneity between the regions investigated, both in terms of structural organization and function. This may suggest that CB2 is predominantly expressed by cells with a supporting role in the CNS, rather than cells with a highly specialized role. Although subtle differences in terms of density and phenotype are beginning to be identified in certain brain regions, microglial cells are present throughout the nervous system and play a crucial homeostatic role [34–36]. Furthermore, CB2 is known to be mostly expressed at the periphery by leukocytes, including myeloid monocytes and macrophages [1, 37, 38], leading to the hypothesis that microglia may be one of the main cells expressing CB2 in the CNS.

In the present study, we firstly used MACS to investigate CB2 expression in enriched populations sorted from adult mouse brain. The MACS technique enabled to obtain interesting yields needed for downstream transcript analysis, in a short space of time. We showed that CB2 was expressed in the brain mostly by CD11b-positive microglial cells, and to a lesser extent by neurons, under basal conditions. This is in agreement with previous measurements in FACS-sorted mouse cortical neurons and microglia [39]. In that study, the difference in CB2 expression between neurons and microglia was even greater than that observed in the current study, maybe due to an activation of microglia during the dissociation and FACS protocol, that might have resulted in induced CB2 expression.

MACS enrichment, based on the use of a single cell marker, is not sufficient by itself to distinguish subpopulations present in a heterogeneous population. Having verified that CB2 expression in the neocortex and hippocampus of 10-day-old mice was identical to that of adult mice, we used data from the analysis of single nuclei from the cortex of 10-day-old mice to gain a better understanding of how cells expressing CB2-mRNA are distributed in the neocortex. These data indicate that, under basal conditions, less than 1% of cortical cells express CB2. Furthermore, this analysis revealed that microglia constituted the cell population with the highest proportion of CB2-positive cells, in line with our MACS results obtained in adult mice.

These results provide new insight on cells involved in physiological and behavioral outcomes observed following pharmacological activation of CB2 in healthy mice. Neuronal CB2 may directly modulate behavioral outcomes [4, 5]. Microglia has been shown to have an indirect role on neuronal activity and in the regulation of behavioral outcomes [40]. Microglial CB2 may thus be in part responsible for some outcomes reported at the physiological state.

CB2 expression in activated microglia

Numerous studies have presented CB2 as a molecule to target in microglial cells/monocytes in different models of pathological conditions to efficiently resolve neuroinflammation [5, 7, 41, 42]. In addition, while CB2 transcript level has been found to be increased in many pathological conditions at the brain tissue level [20, 43–46], it has been speculated that this induction mainly occurred in microglial cells [20, 45, 47]. We have provided strong evidence that CB2 expression is inversely regulated by LPS-induced inflammatory state, both at tissue level, in microglial cells sorted from brain tissue and in the BV2 microglial cell line, and is induced during the resolution phase of inflammation, rather than the inflammatory peak. These results are consistent with the few studies that have demonstrated that CB2 transcript levels are downregulated in microglia cell lines stimulated with LPS [19, 20] or LPS + IFNγ [21, 48]. However, they contrast with the general idea that CB2 is induced in the brain in many pathological models involving neuroinflammation [7, 9]. One potential explanation is the distinct nature of the inflammatory stimulus, which, by engaging various intracellular pathways, may lead to different effects on the regulation of CB2 expression. A previous study demonstrated that the stimulation of BV2 cells with IFNγ leads to an opposite regulation of CB2 expression when compared to the effect induced by LPS. However, the inflammatory responses elicited by LPS and IFNγ were not assessed, rendering it challenging to ascertain whether this discrepancy stemmed from variations in the intensity of inflammation or the characteristics of the inflammatory response [20]. LPS mimics non-sterile inflammation by activating the Toll like receptor 4 (TLR4) and numerous subsequent intracellular pathways including NF-κB [49], and IFNγ models sterile inflammation and binds to the interferon-gamma receptor (IFNGR) protein complex, which activates intracellular JAK/STAT pathways [50]. In this study, we showed that CB2 transcript levels exhibited an inverse regulation in BV2 cells when stimulated with a similar dose of LPS and IFNγ. We demonstrated that BV2 cells exhibited distinct responses to LPS and IFNγ, with differences in terms of the temporal pattern, magnitude, and cytokine profile. The inflammatory response triggered by IFNγ exhibited a slower onset, lower magnitude, and did not result in

an upregulation of IL-1β transcript levels. To investigate whether the substantial decrease in CB2 mRNA levels, observed exclusively with LPS treatment, was a consequence of potent IL-1R activation by IL-1β, we stimulated BV2 cells with LPS in the presence of the natural IL-1R antagonist IL-1RA. Interestingly, we observed no difference in the LPS-induced decrease in CB2 mRNA levels, suggesting that LPS-induced CB2 downregulation is not driven by IL-1β. Subsequent investigations are necessary to clarify these mechanisms.

It is worth noting that the upregulation of CB2 transcripts observed in the brain in several experimental models linked to neuroinflammatory processes could also be attributed to the infiltration of circulating leukocytes, which are known to exhibit robust CB2 expression [1], into the brain parenchyma. Notably, substantial upregulation of CB2 at the transcriptional level has been documented in brain tissue from rodent models of stroke [46], traumatic brain injury [43] or Parkinson's disease [44, 45], for which strong leukocyte infiltration has been reported [43, 51–54].

Conclusion

These results represent a significant advance in our understanding of CB2 expression and the role it might play in the CNS, in both physiological and pathological conditions. Our findings highlight the fact that CB2 expression can be differently regulated in distinct inflammatory environments. It is therefore mandatory to measure CB2 expression in each experimental model before considering pharmacological interventions, with the view to identifying precise target cells and optimal therapeutic windows.

Methods

Full details of the methods are given in the supplementary material.

Experimental design

Experiment 1. To assess mRNA level of CB2, CB1, GPR55 and GPR18 in different mouse strains and brain regions, brains from adult male Balb/c, C57Bl/6 and Swiss mice (n = 3–4/group) were collected after transcardiac perfusion of saline. Olfactory bulbs, neocortices, hippocampi, hypothalamus, cerebellum and brainstem from 9 mice (3/strain) were microdissected. Ventral limbic regions (comprising the piriform cortex, the amygdala and the insular agranular cortex), nuclei accumbens, substantia nigra, striatum and ventral tegmental areas were microdissected from 12 other mice (4/strain). All microdissections were performed on ice and samples were then quickly flash-frozen in liquid nitrogen. Transcript levels were determined by RT-qPCR.

Experiment 2. To validate the efficacy of transcription and translation inhibitors in limiting ex vivo microglial cell activation induced during tissue dissociation and magnetic sorting, the protocol was run in parallel using 3 different buffer conditions applied to all steps of the protocol, from intracardiac perfusion to collection of sorted cells. Experiment was performed on adult C57Bl/6 male mice (n = 2/buffer condition). Transcript levels of inflammatory genes were determined by RT-qPCR.

Experiment 3. To determine in which brain cell types CB2 is expressed under physiological state, brains of C57Bl/6 mice were collected after transcardiac perfusion of the buffer selected in experiment 2 (n = 3). Neocortices and hippocampi were microdissected on ice and immediately processed for magnetic cell separation. Transcript levels were determined by RT-qPCR. Furthermore, a single-nucleus database obtained from cortex tissue collected from 10-day-old mice was used to estimate the proportion of CB2-expressing cells in each cell population.

Experiment 4. To measure the effect of inflammation on CB2 expression in brain microglia, adult C57Bl/6 mice were treated intra-peritoneally (IP) with LPS (*Escherichia coli* O55:B5, Sigma, L2880) at 5 mg/kg and brains were collected 3h (n = 5) or 24 h (n = 5) later after transcardiac perfusion of saline. Mice treated with 0.9% NaCl were used as controls (n = 4). Neocortices and hippocampi were microdissected on ice. Transcript levels were determined by RT-qPCR.

Experiment 5. To investigate CB2 expression in microglial cells under physiological and inflammatory condition, murine BV2 cells were cultured with or without LPS (100 ng/mL) or IFNγ (100 ng/mL) and harvested 1h-24h later for further RT-qPCR analysis (CTRL, LPS + 1 h, + 2 h, + 4 h: 4 wells/condition; LPS + 8 h, + 24 h: 3 wells/condition; CTRL, IFNγ + 3h, + 8h, + 24h: 3 wells/condition). To determine the role of IL-1R signaling in regulating CB2 expression, BV2 cells incubated with LPS (100 ng/mL) were pre-treated for 30 min and co-cultured for 2 h with IL1-RA, before harvesting and further RT-qPCR analysis.

Animals

Adult male mice (Balb/c, C57Bl/6 and Swiss, 8-weeks-old, Envigo, France) were used in this study. The experimental procedures were conducted in accordance with the European Community guidelines for care in animal research and approved by the CELYNE local Ethics Research Committee (protocol #24302). Every effort was made to minimize animal suffering.

BV2 cell culture

The immortalized murine BV2 cell line (BV2 cells) was kindly provided by Dr. Nadia Soussi (NeuroDiderot, Paris University). Cells at passage 9–15 were treated with LPS (from *Escherichia coli* O55:B5, 100 ng/mL, Sigma #L6529) or with IFNγ (100 ng/mL, Gibco #PMC4031) for the indicated time, and harvested for further RT-qPCR analysis. Blockade of IL-1R was performed using the recombinant mouse IL1-RA protein (1–1000 mg/mL, abcam #ab283475).

Reverse transcription and real-time quantitative PCR

After extraction, total RNAs were reverse transcribed to complementary DNA (cDNA) using both oligo dT and random primers with PrimeScript RT Reagent Kit (Takara, #RR037A) according to manufacturer's instructions in the presence of a synthetic external non-homologous poly(A) standard messenger RNA (SmRNA; A. Morales and L. Bezin, patent WO2004.092414) to normalize the RT step, as previously described [55]. Each cDNA of interest was amplified using the Rotor-Gene Q thermocycler (Qiagen), the SYBR Green PCR kit (Qiagen, #208052) and oligonucleotide primers (Eurogentec) specific to the targeted cDNA. cDNA copy number detected was determined using a calibration curve, and results were expressed as cDNA copy number/µg tot RNA.

Pro-inflammatory index (PI-I) was calculated using a specific set of pro-inflammatory genes: IL-1β, IL-6, TNFα, COX2, NOS2 and MPC1. For each sample, the number of copies of each transcript has been expressed in percent of the averaged number of copies measured in the whole considered group of samples. Once each transcript was expressed in percent, an index was calculated by adding the percent of each transcript involved in the composition of the index and expressed in arbitrary units (A.U.), using the formula given in the supplementary material.

Brain dissociation and magnetic cell sorting (MACS studies)

To prevent any artifactual ex vivo gene expression changes during brain dissociation and cell sorting procedures, all buffers and solutions used during the process (from animal perfusion to sorted cells flash freezing) were supplemented with a cocktail composed of Actinomycin D (3 µM, Tocris #1229/10), Anisomycin (100 µM, Tocris #1290/50) and Triptolide (10 µM, Tocris #3253/10)[18]. All steps were performed on ice or using pre-chilled refrigerated centrifuge set to 4 °C with all buffers/solutions pre-chilled before addition to samples to further limit cell activation. The general workflow of brain dissociation and magnetic cell sorting is illustrated in supplementary data (Fig. S1).

Neocortices and hippocampi were quickly dissected, cut in smaller pieces and processed for dissociation using Miltenyi's Adult Brain Dissociation Kit (#130-107-677) according to manufacturer's instruction. To enhance cell yields, distinct mice were used for the isolation of neurons (n = 3) and for the isolation of the other cell types (microglia, endothelial cells and astrocytes, n = 3). Neurons were enriched using Adult Neuron Isolation Kit (Miltenyi #130-126-602). Endothelial cells, microglia and astrocytes were magnetically sorted successively, using the anti-Ly-6C biotin antibody (Miltenyi #130-111-914) and Anti-Biotin MicroBeads (Miltenyi #130-090-485), the CD11b MicroBeads (Miltenyi #130-093-634), and the ACSA-2 MicroBeads (Miltenyi #130-097-679), respectively. Sorted cells were counted manually, spun and dry cell pellets were flash frozen and stored at − 80 °C.

Flow cytometry

To control purity of enriched cell populations, a fraction of cell suspensions was collected before and after each sorting. The following antibodies were added to cell suspensions at 1:50 concentration in B2 buffer: ACSA2-APC (Miltenyi #130-116-245), CD11b-PE Vio770 (Miltenyi #130-113-808), CD31-PE (Miltenyi #130-111-540), Ly6C-APC Vio770 (Miltenyi #130-111-919) and O4-VioBright515 (Miltenyi #130-120-102). DAPI (2.5 µg/mL, Sigma #D9542) was added as a viability marker right before flow cytometry analysis. Cells were analyzed with the BD FACS Canto II Flow Cytometer (Becton–Dickinson) and data files with FlowJo software V10.7.2 (Becton–Dickinson).

Brain dissociation and single nucleus RNAseq (single nucleus study)

Tissue dissociation

Nuclei from whole cortex were obtained from one mouse at age P10, anesthetized with isoflurane and sacrificed by decapitation. The dissected cortex tissue was immediately placed in a dry-ice-cold tube for immediate freezing until processing for nuclei isolation.

Single-nucleus isolation

Dissected frozen cortex was resuspended and mechanically homogenized using dounce homogeneizer to release nuclei following the Salty EZ 10 protocol (dx.doi.org/https://doi.org/10.17504/protocols.io.bx64prgw). Dissected frozen cortex was resuspended into 600µL of cold homogenization buffer that consisted of 10 mM Tris HCl pH 7.5, 146 mM NaCl, 1 mM $CaCl_2$, 21 mM $MgCl_2$, 0.03% Tween 20, 0.01% BSA, 10% EZ buffer (Sigma) and 0.2 U/µL Protector RNase Inhibitor (Roche). Tissues

were then transferred into 2 mL dounce (Kimble) and homogenized using 10 strokes of the loose pestle followed by 8 strokes of the tight pestle to release nuclei, on ice. Homogenate was then strained through a 70 µm cell strainer (Pluriselect) and centrifuged at 500 g for 5 min to pellet nuclei. After removing supernatant, nuclei were washed in 1 ml resuspension buffer containing 10 mM Tris HCl pH 7.5, 10 mM NaCl, 3 mM $MgCl_2$, 1% BSA and 0.2 U/µL Protector RNase Inhibitor and centrifuged at 500xg for 5 min. Nuclei were then resuspended in 500µL of resuspension buffer and 5.10^5 of the best singlet nuclei were sorted (BD ARIA) based on DAPI intensity before counting using the LUNA automated cell counter. Nuclei were finally centrifuged at 500xg for 5 min and diluted in resuspension buffer to a concentration of 1200 nuclei/µl before encapsulation in 10×Chromium. All steps were carried on ice or at 4 °C.

Single-nucleus capture and sequencing

Single-nuclei capture and sequencing were performed at the Cancer Genomics Platform of the Cancer Research Center of Lyon (CRCL). Nuclei suspension (1200 nuclei/µL) were loaded onto a Chromium iX (10X Genomics) to capture 10,000 single nuclei. cDNA synthesis and library preparation were done following the manufacturer's instructions (chemistry V3.1) and library has been sequenced using the Novaseq 6000 (Illumina) to reach 30 k reads per nucleus. Cell Ranger version 6.1.1 (10X Genomics) was used to align reads on the mouse reference genome gex-mm10-2020-A and to produce the count matrix.

Single-nucleus RNA-seq data analysis

The gene expression matrices from Cell Ranger were used for downstream analysis using the software R (version 4.1.2) and the R toolkit Seurat (version 4.1.0). Nuclei were excluded from downstream analysis when they had more than 3% mitochondrial genes, fewer than 300 unique genes, more than 20,000 unique molecular identifiers (UMIs) and detected as doublets using scdblFinder R package. A total of 8530 cells were selected. Gene expression was normalized using the standard Seurat workflow and the 2000 most variable genes were identified and used for principal component analysis (PCA). The top most significant principal components (PCs) were selected for generating the UMAP, based on the ElbowPlot method in Seurat. Clustering of cells was obtained following Seurat graph-based clustering approach with the default Louvain algorithm for community detection. We then performed differential expression analysis using the FindMarkers function of Seurat with the default Wilcoxon rank sum test and annotated clusters based on expression of marker genes (Fig. S4). We then manually annotated the major classes of cells: Neurons, Microglia, Astrocytes, Oligodendrocytes and vascular cells (Fig. 3H-I).

Statistical analysis

Statistical analyses were performed using Prism 10.0 software (GraphPad, USA). Results are presented as mean ± SEM (standard error of the mean). Differences with a p-value < 0.05 ($p < 0.05$) were considered to be statistically significant. The Shapiro–Wilk test and quantile–quantile plot were used to assess normal distribution of the data. For normal data, the statistical significance was assessed by two-tailed t-test or one-way ANOVA, followed with Tukey's *post-hoc* test for multiple comparisons. For non-normal data, the statistical significance was assessed by Kruskal–Wallis test, followed with Dunn's *post-hoc* test for multiple comparisons.

Abbreviations

ACSA2	Astrocyte cell surface antigen-2
ActD	Actinomycin D
Anis	Anisomycine
AU	Arbitrary units
BS	Brainstem
CB1	Cannabinoid receptor type 1
CB2	Cannabinoid receptor type 2
CD	Cluster of differentiation
cDNA	Complementary DNA
CNS	Central nervous system
COX2	Cyclooxygenase-2
CTRL	Control
GPR	G protein-coupled receptor
HI	Hippocampus
IFNGR	Interferon-gamma receptor
IFNγ	Interferon-gamma
IL-1RA	Interleukin-1 receptor antagonist
IL	Interleukine
IP	Intra-peritoneally
KO	Knock out
LPS	Lipopolysaccharide
MACS	Magnetic activated cell sorting
MCP1	Monocyte chemoattractant protein 1
mRNA	Messenger ribonucleic acid
NAc	Nucleus accumbens
NCX	Neocortex
NOS2	Nitric Oxide Synthase 2
OB	Olfactory bulb
PCA	Principal component analysis
PI-I	Pro-inflammatory index
RNAseq	RNA sequencing
RT-qPCR	Reverse transcription quantitative polymerase chain reaction
SEM	Standard error of the mean
SN	Substantia nigra
TLR4	Toll like receptor 4
TNFα	Tumor necrosis factor α
Trip	Triptolide

UMIs	Unique molecular identifiers
VLR	Ventral limbic region
VTA	Ventral tegmental region

Supplementary Information

The online version contains supplementary material available at https://doi.org/10.1186/s12974-024-03202-8.

Additional file 1.

Acknowledgements
We acknowledge the contribution of SFR Santé Lyon-Est (UAR3453 CNRS, US7 Inserm, UCBL) CyLE cytometry platform facilities, especially Thibault Andrieu and Priscillia Battiston-Montagne for their valuable help. We are grateful for animal care provided by the zootechnicians of the CRNL's animal facility.

Author contributions
LB and WG conceived and designed the study. WG, AR, NG, BG, SR, AB and JB participated in data collection and analysis. GM and CD performed RNAseq single nucleus experiments and analysis. WG, LB and GM interpreted the data. WG drafted the manuscript. LB provided critical revisions. All authors read and approved the final manuscript.

Funding
Nadia Gasmi was granted a PhD fellowship from the Fondation pour la Recherche Médicale. Wanda Grabon was granted a PhD fellowship from France Alzheimer.

Availability of data and materials
All data generated or analysed during this study are included in this published article and its supplementary information files. The single nucleus RNAseq data for this study have been deposited in the GEO database under the accession number GSE247268.

Declarations

Ethics approval and consent to participate
Not applicable.

Consent for publication
Not applicable.

Competing interests
The authors declare that they have no competing interests.

Author details
[1]CNRS UMR5292, Inserm U1028, TIGER Team, Université Claude Bernard Lyon 1, Centre de Recherche en Neurosciences de Lyon, 69500 Bron, France. [2]Epilepsy Institute IDEE, 59 Boulevard Pinel, 69500 Bron, France. [3]CNRS UMR5292, Inserm U1028, Université Claude Bernard Lyon 1, Centre de Recherche en Neurosciences de Lyon, GenCyTi Platform, 69500 Bron, France. [4]Cancer Genomic Platform, Inserm 1052, CNRS 5286, Centre Léon Bérard, Centre de Recherche en Cancérologie de Lyon (CRCL), Université de Lyon, Université Claude Bernard Lyon 1, 69008 Lyon, France. [5]Université Claude Bernard Lyon 1, Bioinformatic Platform of the Labex Cortex, 69008 Lyon, France.

Received: 16 January 2024 Accepted: 12 August 2024
Published online: 19 August 2024

References

1. Galiègue S, Mary S, Marchand J, Dussossoy D, Carrière D, Carayon P, et al. Expression of central and peripheral cannabinoid receptors in human immune tissues and leukocyte subpopulations. Eur J Biochem. 1995;232:54–61.
2. Schatz AR, Lee M, Condie RB, Pulaski JT, Kaminski NE. Cannabinoid receptors CB1 and CB2: a characterization of expression and adenylate cyclase modulation within the immune system. Toxicol Appl Pharmacol. 1997;142:278–87.
3. Turcotte C, Blanchet M-R, Laviolette M, Flamand N. The CB2 receptor and its role as a regulator of inflammation. Cell Mol Life Sci. 2016;73:4449–70.
4. Jordan CJ, Xi Z-X. Progress in brain cannabinoid CB2 receptor research: from genes to behavior. Neurosci Biobehav Rev. 2019;98:208–20.
5. Grabon W, Rheims S, Smith J, Bodennec J, Belmeguenai A, Bezin L. CB2 receptor in the CNS: from immune and neuronal modulation to behavior. Neurosci Biobehav Rev. 2023;150:105226.
6. Onaivi ES. Editorial: unravelling the role of CB2r in neuropsychiatric diseases. Front Psychiatry. 2023. https://doi.org/10.3389/fpsyt.2023.1171959.
7. Komorowska-Müller JA, Schmöle A-C. CB2 receptor in microglia: the guardian of self-control. Int J Mol Sci. 2020. https://doi.org/10.3390/ijms22010019.
8. Atwood BK, Mackie K. CB2: a cannabinoid receptor with an identity crisis. Br J Pharmacol. 2010;160:467–79.
9. Grabon W, Bodennec J, Rheims S, Belmeguenai A, Bezin L. Update on the controversial identity of cells expressing cnr2 gene in the nervous system. CNS Neurosci Ther. 2023. https://doi.org/10.1111/cns.13977.
10. Zhang H, Shen H, Jordan CJ, Liu Q, Gardner EL, Bonci A, et al. CB2 receptor antibody signal specificity: correlations with the use of partial CB2-knockout mice and anti-rat CB2 receptor antibodies. Acta Pharmacol Sin. 2019;40:398–409.
11. Liu Q-R, Canseco-Alba A, Zhang H-Y, Tagliaferro P, Chung M, Dennis E, et al. Cannabinoid type 2 receptors in dopamine neurons inhibits psychomotor behaviors, alters anxiety, depression and alcohol preference. Sci Rep. 2017. https://doi.org/10.1038/s41598-017-17796-y.
12. Zhang H-Y, Gao M, Liu Q-R, Bi G-H, Li X, Yang H-J, et al. Cannabinoid CB2 receptors modulate midbrain dopamine neuronal activity and dopamine-related behavior in mice. Proc Natl Acad Sci U S A. 2014;111:E5007–15.
13. Onaivi ES, Ishiguro H, Gong J-P, Patel S, Perchuk A, Meozzi PA, et al. Discovery of the presence and functional expression of cannabinoid CB2 receptors in brain. Ann N Y Acad Sci. 2006;1074:514–36.
14. Zhang H-Y, Bi G-H, Li X, Li J, Qu H, Zhang S-J, et al. Species differences in cannabinoid receptor 2 and receptor responses to cocaine self-administration in mice and rats. Neuropsychopharmacology. 2015;40:1037–51.
15. Zhang H-Y, De Biase L, Chandra R, Shen H, Liu Q-R, Gardner E, et al. Repeated cocaine administration upregulates CB2 receptor expression in striatal medium-spiny neurons that express dopamine D1 receptors in mice. Acta Pharmacol Sin. 2022;43:876–88.
16. Stempel AV, Stumpf A, Zhang H-Y, Özdoğan T, Pannasch U, Theis A-K, et al. Cannabinoid type 2 receptors mediate a cell type-specific plasticity in the hippocampus. Neuron. 2016;90:795–809.
17. Li Y, Kim J. Neuronal expression of CB2 cannabinoid receptor mRNAs in the mouse hippocampus. Neuroscience. 2015;311:253–67.
18. Ocañas SR, Pham KD, Blankenship HE, Machalinski AH, Chucair-Elliott AJ, Freeman WM. Minimizing the Ex Vivo confounds of cell-isolation techniques on transcriptomic and translatomic profiles of purified microglia. eNeuro. 2022;9:ENEURO.0348-21.2022.
19. Carlisle SJ, Marciano-Cabral F, Staab A, Ludwick C, Cabral GA. Differential expression of the CB2 cannabinoid receptor by rodent macrophages and macrophage-like cells in relation to cell activation. Int Immunopharmacol. 2002;2:69–82.
20. Maresz K, Carrier EJ, Ponomarev ED, Hillard CJ, Dittel BN. Modulation of the cannabinoid CB2 receptor in microglial cells in response to inflammatory stimuli. J Neurochem. 2005;95:437–45.
21. Schmöle A-C, Lundt R, Ternes S, Albayram Ö, Ulas T, Schultze JL, et al. Cannabinoid receptor 2 deficiency results in reduced neuroinflammation in an Alzheimer's disease mouse model. Neurobiol Aging. 2015;36:710–9.
22. Bauermeister K, Burger M, Almanasreh N, Knopf HP, Schumann RR, Schollmeyer P, et al. Distinct regulation of IL-8 and MCP-1 by LPS and interferon-gamma-treated human peritoneal macrophages. Nephrol Dial Transplant. 1998;13:1412–9.
23. Schroder K, Sweet MJ, Hume DA. Signal integration between IFNγ and TLR signalling pathways in macrophages. Immunobiology. 2006;211:511–24.
24. Marsh SE, Walker AJ, Kamath T, Dissing-Olesen L, Hammond TR, de Soysa TY, et al. Dissection of artifactual and confounding glial signatures

by single-cell sequencing of mouse and human brain. Nat Neurosci. 2022;25:306–16.
25. Augusto-Oliveira M, Arrifano GP, Lopes-Araújo A, Santos-Sacramento L, Takeda PY, Anthony DC, et al. What do microglia really do in healthy adult brain? Cells. 2019;8:1293.
26. Paolicelli RC, Sierra A, Stevens B, Tremblay M-E, Aguzzi A, Ajami B, et al. Microglia states and nomenclature: a field at its crossroads. Neuron. 2022;110:3458–83.
27. Bensaude O. Inhibiting eukaryotic transcription. Which compound to choose? How to evaluate its activity? Transcription. 2011;2:103–8.
28. Grollman AP. Inhibitors of protein biosynthesis: II. Mode of action of Anisomycin. J Biol Chem. 1967;242:3226–33.
29. Kruk-Slomka M, Dzik A, Biala G. The influence of CB2-receptor ligands on the memory-related responses in connection with cholinergic pathways in mice in the passive avoidance test. Molecules. 2022;27:4252.
30. García-Gutiérrez MS, Ortega-Álvaro A, Busquets-García A, Pérez-Ortiz JM, Caltana L, Ricatti MJ, et al. Synaptic plasticity alterations associated with memory impairment induced by deletion of CB2 cannabinoid receptors. Neuropharmacology. 2013;73:388–96.
31. Onaivi ES, Ishiguro H, Gong J-P, Patel S, Meozzi PA, Myers L, et al. Brain neuronal CB2 cannabinoid receptors in drug abuse and depression: from mice to human subjects. PLoS ONE. 2008. https://doi.org/10.1371/journal.pone.0001640.
32. Cortez IL, Silva NR, Rodrigues NS, Pedrazzi JFC, Del Bel EA, Mechoulam R, et al. HU-910, a CB2 receptor agonist, reverses behavioral changes in pharmacological rodent models for schizophrenia. Prog Neuropsychopharmacol Biol Psychiatry. 2022;117:110553.
33. Grenald SA, Young MA, Wang Y, Ossipov MH, Ibrahim MM, Largent-Milnes TM, et al. Synergistic attenuation of chronic pain using mu opioid and cannabinoid receptor 2 agonists. Neuropharmacology. 2017;116:59–70.
34. Bridlance C, Thion MS. Multifaceted microglia during brain development: models and tools. Front Neurosci. 2023. https://doi.org/10.3389/fnins.2023.1125729.
35. Tan Y-L, Yuan Y, Tian L. Microglial regional heterogeneity and its role in the brain. Mol Psychiatry. 2020;25:351–67.
36. Dos Santos SE, Medeiros M, Porfirio J, Tavares W, Pessôa L, Grinberg L, et al. Similar microglial cell densities across brain structures and mammalian species: implications for brain tissue function. J Neurosci. 2020;40:4622–43.
37. Munro S, Thomas KL, Abu-Shaar M. Molecular characterization of a peripheral receptor for cannabinoids. Nature. 1993;365:61–5.
38. Graham ES, Angel CE, Schwarcz LE, Dunbar PR, Glass M. Detailed characterisation of CB2 receptor protein expression in peripheral blood immune cells from healthy human volunteers using flow cytometry. Int J Immunopathol Pharmacol. 2010;23:25–34.
39. Liu Q-R, Canseco-Alba A, Liang Y, Ishiguro H, Onaivi ES. Low basal CB2R in dopamine neurons and microglia influences cannabinoid tetrad effects. Int J Mol Sci. 2020;21:9763.
40. Wake H, Moorhouse AJ, Nabekura J. Functions of microglia in the central nervous system—beyond the immune response. Neuron Glia Biol. 2011;7:47–53.
41. Ashton JC, Glass M. The Cannabinoid CB2 receptor as a target for inflammation-dependent neurodegeneration. Curr Neuropharmacol. 2007;5:73–80.
42. Cabral GA, Raborn ES, Griffin L, Dennis J, Marciano-Cabral F. CB2 receptors in the brain: role in central immune function. Br J Pharmacol. 2008;153:240–51.
43. Braun M, Khan ZT, Khan MB, Kumar M, Ward A, Achyut BR, et al. Selective activation of cannabinoid receptor-2 reduces neuroinflammation after traumatic brain injury via alternative macrophage polarization. Brain Behav Immun. 2018;68:224–37.
44. Concannon RM, Okine BN, Finn DP, Dowd E. Differential upregulation of the cannabinoid CB2 receptor in neurotoxic and inflammation-driven rat models of Parkinson's disease. Exp Neurol. 2015;269:133–41.
45. Gómez-Gálvez Y, Palomo-Garo C, Fernández-Ruiz J, García C. Potential of the cannabinoid CB2 receptor as a pharmacological target against inflammation in Parkinson's disease. Prog Neuropsychopharmacol Biol Psychiatry. 2016;64:200–8.
46. Zarruk JG, Fernández-López D, García-Yébenes I, García-Gutiérrez MS, Vivancos J, Nombela F, et al. Cannabinoid type 2 receptor activation downregulates stroke-induced classic and alternative brain macrophage/microglial activation concomitant to neuroprotection. Stroke. 2012;43:211–9.
47. Ashton JC, Rahman RMA, Nair SM, Sutherland BA, Glass M, Appleton I. Cerebral hypoxia-ischemia and middle cerebral artery occlusion induce expression of the cannabinoid CB2 receptor in the brain. Neurosci Lett. 2007;412:114–7.
48. Young AP, Denovan-Wright EM. Synthetic cannabinoids reduce the inflammatory activity of microglia and subsequently improve neuronal survival in vitro. Brain Behav Immun. 2022;105:29–43.
49. Lu Y-C, Yeh W-C, Ohashi PS. LPS/TLR4 signal transduction pathway. Cytokine. 2008;42:145–51.
50. Schroder K, Hertzog PJ, Ravasi T, Hume DA. Interferon-gamma: an overview of signals, mechanisms and functions. J Leukoc Biol. 2004;75:163–89.
51. Alam A, Thelin EP, Tajsic T, Khan DZ, Khellaf A, Patani R, et al. Cellular infiltration in traumatic brain injury. J Neuroinflammation. 2020;17:328.
52. Gao L, Brenner D, Llorens-Bobadilla E, Saiz-Castro G, Frank T, Wieghofer P, et al. Infiltration of circulating myeloid cells through CD95L contributes to neurodegeneration in mice. J Exp Med. 2015;212:469–80.
53. Kronenberg G, Uhlemann R, Richter N, Klempin F, Wegner S, Staerck L, et al. Distinguishing features of microglia- and monocyte-derived macrophages after stroke. Acta Neuropathol. 2018;135:551–68.
54. Rajan WD, Wojtas B, Gielniewski B, Gieryng A, Zawadzka M, Kaminska B. Dissecting functional phenotypes of microglia and macrophages in the rat brain after transient cerebral ischemia. Glia. 2019;67:232–45.
55. Morales A, Bonnet C, Bourgoin N, Touvier T, Nadam J, Laglaine A, et al. Unexpected expression of orexin-B in basal conditions and increased levels in the adult rat hippocampus during pilocarpine-induced epileptogenesis. Brain Res. 2006;1109:164–75.

Publisher's Note